Table 2 Simultaneous repeatability of highly sensitive HbsAg chemiluminescent enzyme immunoassay (prototype) (6 times examination)

Samples	Coefficient of variation (%)
LL	3.2
L	2.8
M	1.7
H	1.9
HH	5.0

Table 4 Specificity of highly sensitive HBsAg chemiluminescent enzyme immunoassay (prototype)

Value (mIU/ml)	n
0	217
1	5
2	2
3	0
4	2
5.0≦	0
total	226

Table 3 Daily repeatability of highly sensitive HBsAg chemiluminescent enzyme immunoassay (prototype) (6 days measurement)

Samples	date						
	Sep 14th 2009	Sep 15th 2009	Sep 16th 2009	Sep 17th 2009	Sep 18th 2009	Sep 24th 2009	Coefficient of variation (%)
LL	47.7	53.7	54.0	55.4	51.2	48.9	5.9
L	538.5	524.9	566.1	580.3	546.4	500.7	5.3
M	6,413.3	6,481.9	6,490.8	6,457.4	6,579.8	5,936.9	3.6
H	56,872.0	57,030.6	56,762.1	59,069.5	57,932.6	55,353.7	2.2
HH	342,672.5	358,378.4	391,019.9	373,374.9	380,694.8	372,547.0	4.6

Table 5 The comparison of highly sensitive HBsAg chemiluminescent enzyme immunoassay (prototype) with Abbott ARCHITECT

		Highly sensitive HBsAg chemiluminescent enzyme immunoassay		
		positive	negative	total
Abbott ARCHITECT	positive	47	0	47
	negative	2	10	12
	total	49	10	59

最大 5.9%と良好な再現性であった(**Table 3**)。

B. 特異性試験

226 例の HBs 抗原陰性検体(うち 118 例が抗 HCV 抗体陽性検体)を使用して特異性試験を行ったところ測定値はすべて 5mIU/ml 未満であり特異度は 100%であった(**Table 4**)。

C. 従来法との比較

以前に B 型肝炎と診断された患者血清 59 検体を用いて，従来の HBs 抗原定量測定法としてアーキテクト HBsAg-QT との相関を確認した。本試薬とアーキテクト HBsAg-QT との両者の判定一致率は 96.6%であった。うち 2 検体においてアーキテクト HBsAg-QT にて陰性で，本試薬にて陽性であった。その 2 検体に関しては本試薬にて 10.2mIU/ml，14.8mIU/ml とアーキテクト HBsAg-QT の検出限界である 50mIU/ml 未満であり，HBs 抗原定量試薬の高感度化により検出可能となった(**Table 5**)。本試薬とアーキテクト HBsAg-QT との相関を検討した。アーキテクト HBsAg-QT にて HBs 抗原陽性であった 47 サンプルにて検討したところ，相関傾きは若干高かったものの，相関係数は良好であった(y＝1.4911x−1,435,268，r＝0.953)(**Fig. 2a**)。なお，低値域 41 サンプルについて検討したところ，相関係数はより良好であった(y＝1.0895x−38,242，r＝0.977)(**Fig. 2b**)。

D. HBV DNA TaqMan PCR との比較

以前に B 型肝炎と診断された患者血清 58 検体を用いて本試薬による HBs 測定と HBV DNA TaqMan

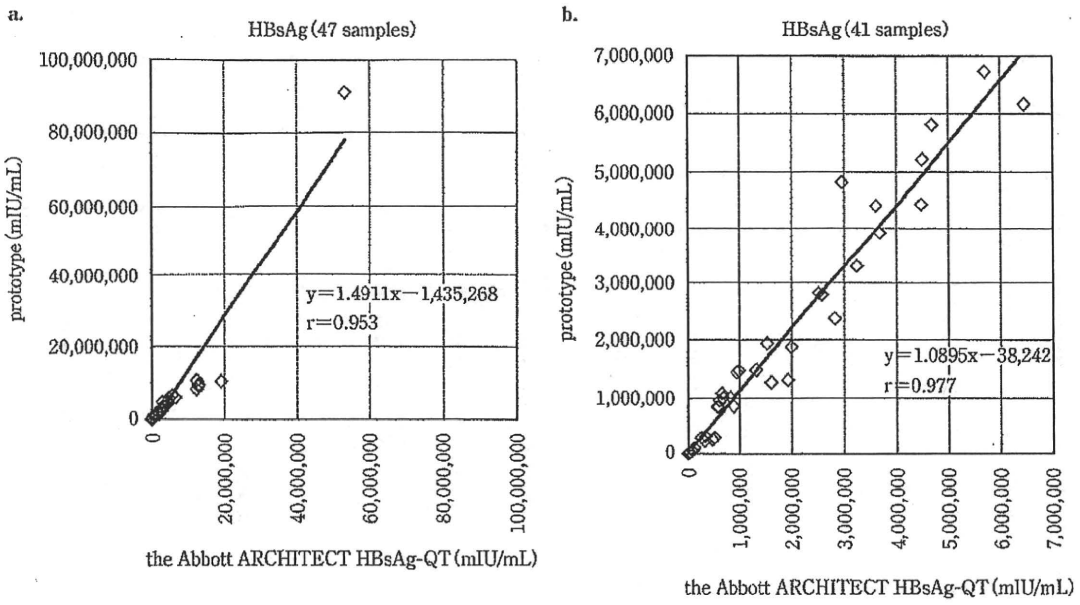

Figure 2

a. Correlation for HBsAg of serum samples between prototype and the Abbott ARCHITECT HBsAg-QT.

b. Correlation for HBsAg of serum samples between prototype and the Abbott ARCHITECT HBsAg-QT (low value).

Table 6 The comparison of highly sensitive HBsAg chemiluminescent enzyme immunoassay (prototype) with HBV DNA Taqman PCR

		highly sensitive HBsAg chemiluminescent enzyme immunoassay (prototype)		
		positive	negative	total
HBV DNA TaqMan PCR	positive	24	1	25
	under detectable limit	6	0	6
	negative	18	9	27
	total	48	10	58

PCR(コバス TaqMan HBV「オート」(ロシュ・ダイアグノスティックス株式会社))それぞれにおいて相関性を比較した。判定一致率は 67.2%であった。HBV DNA Taqman PCR で陰性のもの 27 サンプル中 18 サンプルで本試薬において陽性であった(**Table 6**)。

実際の症例を提示する：症例 1：55 歳男性，ALT は 23 IU/L，HBV-DNA は TMA 法で 3.7 LGE/ml 未満，HBe 抗原陰性，HBe 抗体陽性であった。経過観察中に核酸アナログの投与はしていない。ALT は経過中正常値のままであった。HBV-DNA は最終的に TaqMan 法にても陰性化した。経時的に HBs 抗原を経過観察したところ，本試薬とアーキテクト HBsAg-QT の両者において類似の推移を示した(**Fig. 3a**)。症例 2：60 歳男性，ALT は 55 IU/L と軽度上昇，HBV-DNA は TMA 法で 3.7 LGE/ml 未満，HBe 抗原陰性，HBe 抗体陽性であった。経過観察中に核酸アナログの投与はしていない。経過観察中に HBV DNA はアンプリコア法でも測定したが検出感度未満であった。経過中に ALT は一時 122 IU/ml まで上昇したが，その後は改善した。HBs 抗原は持続的に減少し，アーキテクト HBsAg-QT の検出感度以下になったが，その時点において本試薬では HBs 抗原の定量をすることが可能であった(**Fig. 3b**)。

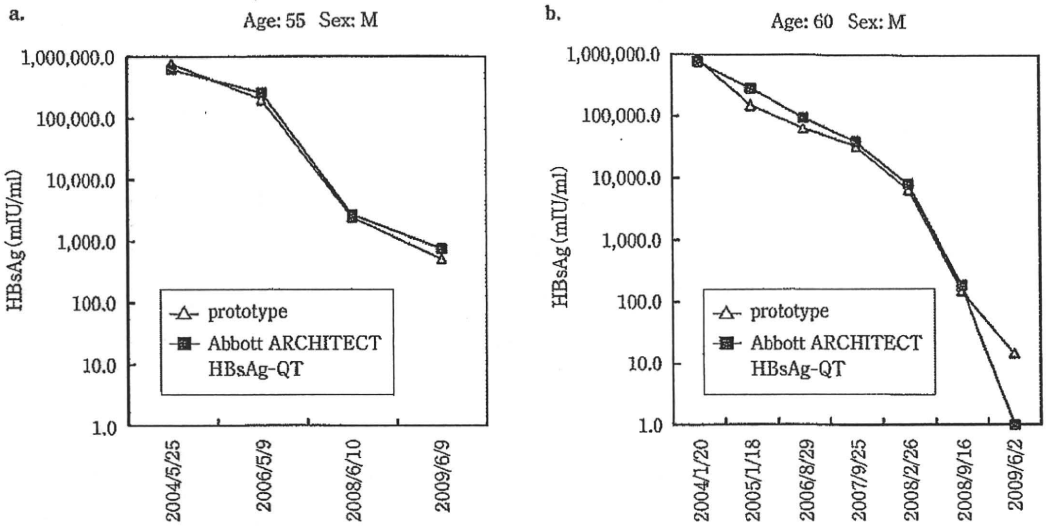

Figure 3

a. Prototype and the Abbott ARCHITECT HBsAg-QT changes over time in one chronic hepatitis B patient.

b. Prototype and the Abbott ARCHITECT HBsAg-QT changes over time in one chronic hepatitis B patient with HBsAg seroconversion.

III. 考　　察

本試薬は，HBV エンベロープを破壊し，HBs 抗原を遊離させることで検出感度を向上させている。しかしながらそれによって本来 HBV 粒子（Dane 粒子）上の HBs 抗原のみならず Dane 粒子の 10,000～1,000,000 倍以上存在すると言われている，ウイルス DNA の存在しない小型球状粒子上の small S 蛋白を検出することで，従来法と本試薬との間でデータが大きく乖離する懸念があったが，**Fig. 2a, b** に示したようにアーキテクト HBsAg-QT との相関は良好であり，かつ，従来法よりも感度が 10 倍向上し検出限界が 5mIU/ml になったことで **Fig. 3a, b** に示したように HBs 抗原をより低値まで追跡可能であった。また，自動化することにより PCR 法を用いた HBV-DNA 定量より簡便で，しかも安価な検査であることから実際の臨床の場で汎用されることが期待される。高感度で迅速検査にも対応可能となり，HBV 感染を疑う重症肝炎患者など緊急を要する場合においても有用であると考えられる。

最近，HBc 抗体あるいは HBs 抗体陽性の既往感染者からの HBV 再活性化に伴う劇症肝炎の報告が散見されている[7)~9)]。特に，リツキシマブ＋ステロイドを含む化学療法後に肝炎を発症する頻度は比較的高く，ガイドラインでは HBV-DNA のモニタリングが推奨されている[10)]。確かに HBV-DNA 定量は非常に有用な手段であるが，高価かつ煩雑であり，今回提示した本試薬の感度がさらに向上すれば，HBV-DNA 定量に代わる検査となり得るかもしれない。また，従来の HBs 抗原検出系においては一次抗体が HBs 抗原の外側エピトープ認識抗体を使用していた。近年，“a” determinant におけるワクチンエスケープ変異が報告されており[11)~13)]，従来の HBs 抗原検出系では検出感度の低下が指摘されている[14)]。今回の本試薬は内側リニア認識抗体も一次抗体に使用することで，そうした懸念を解消するかもしれない。

IV. 結　　語

新しい検査試薬である超高感度 HBs 抗原定量試薬はその高感度と即時性において臨床応用が期待される。

文　　献

1) Lok AS. Chronic hepatitis B. New Engl J Med 2002; 346: 1682-3.

2) Wursthorn K, Lutgehetmann M, Dandri M, et al. Peginterferon alpha-2b plus adefovir induce strong cccDNA decline and HBsAg reduction in patients with chronic hepatitis B. Hepatology 2006; 44: 675–84.
3) Brunetto MR, Moriconi F, Bonino F, et al. Hepatitis B virus surface antigen levels: a guide to sustained response to peginterferon alfa-2a in HBeAg-negative chronic hepatitis B. Hepatology 2009; 49: 1141–50.
4) Chen CH, Lee CM, Wang JH, et al. Correlation of quantitative assay of hepatitis B surface antigen and HBV DNA levels in asymptomatic hepatitis B virus carriers. Eur J Gastroenterol Hepatol 2004; 16: 1213–8.
5) Deguchi M, Yamashita N, Kagita M, et al. Quantitation of hepatitis B surface antigen by an automated chemiluminescent microparticle immunoassay. J Virol Methods 2004; 115: 217–22.
6) Matsubara N, Kusano O, Sugamata Y, et al. A novel hepatitis B virus surface antigen immunoassay as sensitive as hepatitis B virus nucleic acid testing in detecting early infection. Transfusion 2009; 49: 585–95.
7) Law JK, Ho JK, Hoskins PJ, et al. Fatal reactivation of hepatitis B post-chemotherapy for lymphoma in a hepatitis B surface antigen-negative, hepatitis B core antibody-positive patient: potential implications for future prophylaxis recommendations. Leuk Lymphoma 2005; 46: 1085–9.
8) Fukushima N, Mizuta T, Tanaka M, et al. Retrospective and prospective studies of hepatitis B virus reactivation in malignant lymphoma with occult HBV carrier. Ann Oncol 2009; 20: 2013–7.
9) Wu JM, Huang YH, Lee PC, et al. Fatal reactivation of hepatitis B virus in a patient who was hepatitis B surface antigen negative and core antibody positive before receiving chemotherapy for non-Hodgkin lymphoma. J Clin Gastroenterol 2009; 43: 496–8.
10) 坪内 博, 熊田 博, 清澤 研, 他. 免疫抑制・化学療法により発症するB型肝炎対策 厚生労働省「難治性の肝・胆道疾患に関する調査研究」班劇症肝炎分科会および「肝硬変を含めたウイルス性肝疾患の治療の標準化に関する研究」班合同報告. 肝臓 2009; 50: 38–42.
11) Ly TD, Servant-Delmas A, Bagot S, et al. Sensitivities of four new commercial hepatitis B virus surface antigen (HBsAg) assays in detection of HBsAg mutant forms. J Clin Microbiol 2006; 44: 2321–6.
12) Carman WF. The clinical significance of surface antigen variants of hepatitis B virus (Suppl 1). J Viral Hepat 1997; 4: 11–20.
13) Gerlich WH. Diagnostic problems caused by HBsAg mutants-a consensus report of an expert meeting. Intervirology 2004; 47: 310–3.
14) Coleman PF. Detecting hepatitis B surface antigen mutants. Emerg Infect Dis 2006; 12: 198–203.

Cancer Immunol Immunother (2010) 59:453–463
DOI 10.1007/s00262-009-0764-x

ORIGINAL ARTICLE

Natural killer cell is a major producer of interferon γ that is critical for the IL-12-induced anti-tumor effect in mice

Akio Uemura · Tetsuo Takehara · Takuya Miyagi · Takahiro Suzuki · Tomohide Tatsumi · Kazuyoshi Ohkawa · Tatsuya Kanto · Naoki Hiramatsu · Norio Hayashi

Received: 12 February 2009 / Accepted: 24 August 2009 / Published online: 16 September 2009

Abstract Although the anti-tumor effect of IL-12 is mediated mostly by IFNγ, which cell types most efficiently produce IFNγ and therefore initiate or promote the anti-tumor effect of IL-12 has not been clearly determined. In the present study, we demonstrated hydrodynamic injection of the IL-12 gene led to prolonged IFNγ production, NK-cell activation and complete inhibition of liver metastasis of CT-26 colon cancer cells in wild-type mice, but not in IFNγ knockout mice. NK cells expressed higher levels of STAT4 and upon IL-12 administration displayed stronger STAT4 phosphorylation and IFNγ production than non-NK cells. Adoptive transfer of wild-type NK cells into IFNγ knockout mice restored IL-12-induced IFNγ production, NK-cell activation and anti-tumor effect, whereas transfer of the same number of wild-type non-NK cells did not. In conclusion, NK cells are predominant producers of IFNγ that is critical for IL-12 anti-tumor therapy.

Keywords IFNγ · Innate immunity · Liver tumor · IL-12 · NK

A. Uemura and T. Takehara contributed equally to this work.

Electronic supplementary material The online version of this article (doi:10.1007/s00262-009-0764-x) contains supplementary material, which is available to authorized users.

A. Uemura · T. Takehara · T. Miyagi · T. Suzuki · T. Tatsumi · K. Ohkawa · T. Kanto · N. Hiramatsu · N. Hayashi (✉)
Department of Gastroenterology and Hepatology,
Osaka University Graduate School of Medicine,
2-2 Yamada-oka, Suita, Osaka 565-0871, Japan
e-mail: hayashin@gh.med.osaka-u.ac.jp

A. Uemura
e-mail: akioue@gh.med.osaka-u.ac.jp

Introduction

IL-12 is a 70-kDa heterodimer protein, composed of p35 and p40 subunits, mainly produced by antigen-presenting cells. IL-12 was originally found as a "natural killer-stimulating factor" and a "cytotoxic lymphocyte maturation factor" [1, 2]. IL-12 has multi-potent effects, inducing a Th1 response, enhancing the CD8 T-cell response, activating natural killer cells and inducing production of IFNγ [3, 4]. Therapeutic use of IL-12, either using its recombinant protein or gene, can induce an efficient anti-tumor effect on primary or metastatic tumors in various murine models and humans [5, 6].

Research has shown that IL-12 mediates anti-tumor effects in a variety of ways. They include anti-proliferative effects, anti-angiogenic effects [7, 8] and cytotoxic effects of effector lymphocytes. A variety of effector cells has been reported to be required for IL-12-mediated anti-tumor effects: they include CD8 T cells [9], NKT cells [10], CD4 T cells [11] and NK cells [12]. The relative contribution of these cells may differ among IL-12 doses and types of tumor models [13]. Endogenous IFNγ production is required for most, if not all, of the anti-tumor effects of IL-12 administration [14, 15]. IL-12 stimulates a variety of immune cells, such as T cells [16], B cells [17] and NK cells [18], to produce IFNγ. However, which cell types are most critical for producing IFNγ during IL-12 therapy is not clearly known.

In the present study, we used a murine model of liver metastasis of CT-26 colon cancer cells and found that NK cells highly expressed the IL-12 signaling molecule STAT4 and most efficiently produced IFNγ. IFNγ was essential for the anti-tumor effect of IL-12, and NK-cell production of IFNγ sufficed to produce the full-blown anti-tumor effects. These results demonstrated that NK cells

serve not only as an effector but also as an important mediator producing IFNγ that is critical for the anti-tumor effects of IL-12.

Materials and methods

Mice

Specific pathogen-free female Balb/c mice were purchased from Clea Japan, Inc (Tokyo, Japan). Rag2 knockout (Rag2 KO) mice with a Balb/c background were purchased from Taconic (Germantown, NY). IFNγ knockout (GKO) mice with a Balb/c background were kindly provided by Dr. Yoichiro Iwakura (Institute of Medical Science, University of Tokyo). All mice used were at the age of 6 to 10 weeks. They were housed under conditions of controlled temperature and light with free access to food and water at the Institute of Experimental Animal Science, Osaka University Graduate School of Medicine. All animals received humane care, and the study protocol complied with the institution's guidelines.

Tumor models

Intra-splenic injection of tumor cells was used to establish micro-disseminated liver tumors in mice [19]. CT-26 colon cancer cells originating from Balb/c mice were maintained in RPMI1620 supplemented with 10% FCS. Syngeneic mice were anesthetized with pentobarbital and given a cut on the left side flank. CT-26 cells (1×10^5) were suspended in 200 μl of PBS and injected into the spleen.

Injection of naked plasmid DNA

A plasmid coding the murine IL-12 gene, pCMV-IL-12, was generously provided by Dr. M Watanabe (Laboratory of Experimental Immunology, Division of Basic Sciences, National Cancer Institute-Frederick Cancer Research and Development Center) [20]. Plasmid DNA was prepared using an EndoFree plasmid system (Qiagen, Hilden, Germany,) according to the manufacturer's instructions. Hydrodynamic injection of plasmid DNA was performed as previously described [21]. In brief, 25 μg of plasmid DNA was diluted with 2.0 ml of lactated Ringer's solution and injected into the tail vein, using a syringe with a 26-gauge needle. DNA injection was completed within 5 to 8 s.

ELISA

Blood samples were serially obtained from the venous plexus in the retro-orbita under light anesthesia. The levels of serum IL-12 p70, IFNγ (BD Biosciences-Pharmingen, San Diego, CA), IFNγ-inducible protein 10 (IP-10) and monokine induced by IFNγ (MIG) (R&D Systems, Inc, Minneapolis, MN) were measured using commercially available ELISA kits in accordance with the manufacturer's instructions.

Mononuclear cells

Mononuclear cells were isolated from the liver or spleen as previously described. The NK activity of mononuclear cells was assessed by a standard 4-h ^{51}Cr-releasing assay using Yac1 cells as targets. In some experiments, mononuclear cells were separated into $DX5^+$ cells (NK cells) and $DX5^-$ cells (non-NK cells) using the MACS system (Miltenyi Biotec GmbH, Bergisch Gladbach, Germany). The purity of the isolated NK-cell population was found to be greater than 90% by FACS analysis.

Flow cytometric analysis

Liver mononuclear cells were isolated 2 days after pCMV-IL-12 injection. Cytokine secretion was then blocked by the addition of brefeldin A for 4 h. Next, liver mononuclear cells were stained with FITC-conjugated anti-TCRβ antibody and biotin-conjugated anti-CD49b antibody (DX5), fixed and permeabilized with Cytofix/Cytoperm (BD Biosciences), and stained with PE-conjugated anti-INFγ antibody or corresponding isotype controls. Analysis was performed using a FACSCalibur (Becton Dickinson), with the resulting data analyzed using the CELLQuest program (Becton Dickinson). NK cells were identified as $DX5^+/TCR\beta^-$ lymphocytes, NKT cells as $DX5^+/TCR\beta^+$ lymphocytes and T cells as $DX5^-/TCR\beta^+$ lymphocytes.

Adoptive transfer

For adoptive transfer experiments, GKO mice were injected intravenously 1 day before plasmid DNA injection with 2.0×10^8 whole mononuclear cells or 4.0×10^6 NK cells, or non-NK cells or whole mononuclear cells, all of which had been harvested from wild-type mice that can produce IFNγ.

Western blotting

Mouse recombinant IL-12 was purchased from R&D Systems, Inc (Minneapolis, MN). Mononuclear cells were treated with or without IL-12. Whole cell lysate was prepared from mononuclear cells from mice, and 20 μg of protein was separated by SDS-PAGE and transferred to the PVDF membrane. The membrane was stained with anti-STAT4 antibody (BD biosciences),

anti-phospho-specific STAT4 (pY693) antibody (BD biosciences), anti-STAT1 antibody (Cell Signaling), anti-phospho-specific STAT1 antibody (Cell Signaling) and visualized by chemiluminescence.

NK-cell depletion

For depletion of NK cells in vivo, anti-asialoGM1 antibody (WAKO, Osaka, Japan) was intraperitoneally administered. We determined the appropriate dosing to be 500 μg/mouse (50 μl when dissolved according to the manufacturer's instructions) based on FACS analysis of hepatic mononuclear cells. The percentage of $DX5^+/TCR\beta^-$ cells (NK cells) is 12.6 ± 2.4% in IgG-injected liver, whereas it decreased to 0.76 ± 0.04% one day after anti-asialo GM1 antibody injection ($N = 3$/group). This effect remained at least 3 days after anti-asialo GM1 antibody injection. NKT cells were less affected than NK cells, because 90% of $DX5^+/TCR\beta^+$ cells (NKT cells) still remained in the liver after the treatment. Anti-asialoGM1 antibody was injected 1 day after tumor inoculation and then every 5 days. For the control, the same amount of normal rabbit immunoglobulin (DAKO, Copenhagen, Denmark) was intraperitoneally administered.

Histology

The formalin-fixed livers were paraffin-embedded, and liver sections were analyzed by hematoxylin-eosin staining. Acetone-fixed fresh frozen liver sections were immunostained with anti-mouse CD4 (H123.19), anti-mouse CD8α (53-6.7) or anti-CD31 (390) monoclonal antibody (all from BD Biosciences), using a VECSTAIN ABC kit (Vector Laboratories, Burlingame, California, USA).

Statistics

Data are represented as mean ± SD. Comparisons between groups were analyzed by unpaired t-test with Welch's correction. $p < 0.05$ was considered statistically significant.

Results

Hydrodynamic injection of IL-12-expressing plasmid led to prolonged production of IFNγ

Hydrodynamics-based gene delivery into mice establishes efficient foreign gene expression predominantly in the liver, especially in hepatocytes. Serial measurement of serum IL-12 demonstrated that pCMV-IL-12 injection led to substantial IL-12 production on day 1. The levels of serum IL-12 then rapidly declined (Fig. 1a). We also measured IFNγ production in serum, since IL-12 is known to activate IFNγ production. pCMV-IL-12 and, to a lesser extent, pCMV injection increased serum IFNγ on day 1. In contrast to the pCMV injection group, high levels of serum IFNγ were maintained at later time points in the pCMV-IL-12 injection group (Fig. 1a). Thus, hydrodynamic injection of pCMV-IL-12 led to prolonged production of IFNγ. Transient IFNγ production followed by control plasmid may be an indirect effect of liver injury caused by bolus injection of saline or DNA injection.

IL-12 therapy induced NK activation and anti-metastatic effects, both of which are critically dependent on IFNγ

To examine the biological effects of the produced IL-12, we evaluated the NK activity of mononuclear cells from the liver. pCMV-IL-12 injection, but not control pCMV injection, increased Yac1 lytic activity of hepatic mononuclear cells (Fig. 1b). When GKO mice were injected with pCMV-IL-12 or pCMV, the hepatic mononuclear cells did not display any lytic ability to Yac1 cells, suggesting that IL-12-mediated NK-cell activation required IFNγ.

To examine the anti-metastatic effect of IL-12, pCMV-IL-12 or pCMV was injected into wild-type mice 2 days after intrasplenic injection of CT-26 cells. At 14 days after tumor injection, the mice were killed for evaluation of liver tumor (Fig. 1c). While pCMV-injected mice displayed huge liver tumors, pCMV-IL-12-injected mice did not show any macroscopic or microscopic tumor (Fig. 1d). Liver weight was significantly higher in pCMV-injected mice than pCMV-IL-12-injected mice, reflecting liver tumor formation. To examine the involvement of IFNγ in the IL-12-induced anti-tumor effect, we injected pCMV or pCMV-IL-12 into GKO mice 2 days after CT-26 injection. At 14 days after CT-26 injection, both groups showed similar degrees of tumor formation and there was no significant difference in liver weight between the two. This indicated that IL-12-induced anti-metastatic effect was strictly dependent on IFNγ.

NK cells were the most potent producer of IFNγ during IL-12 therapy

To evaluate which cell types most efficiently produced IFNγ, we isolated hepatic mononuclear cells from mice 2 days after plasmid injection and then stained cell surface TCRβ and DX5 as well as intracellular IFNγ (Fig. 2). $TCR\beta^-/DX5^+$ NK cells, $TCR\beta^+/DX5^+$ NKT cells and $TCR\beta^+/DX5^-$ T cells from pCMV-IL-12-injected mice showed significant levels of IFNγ production compared

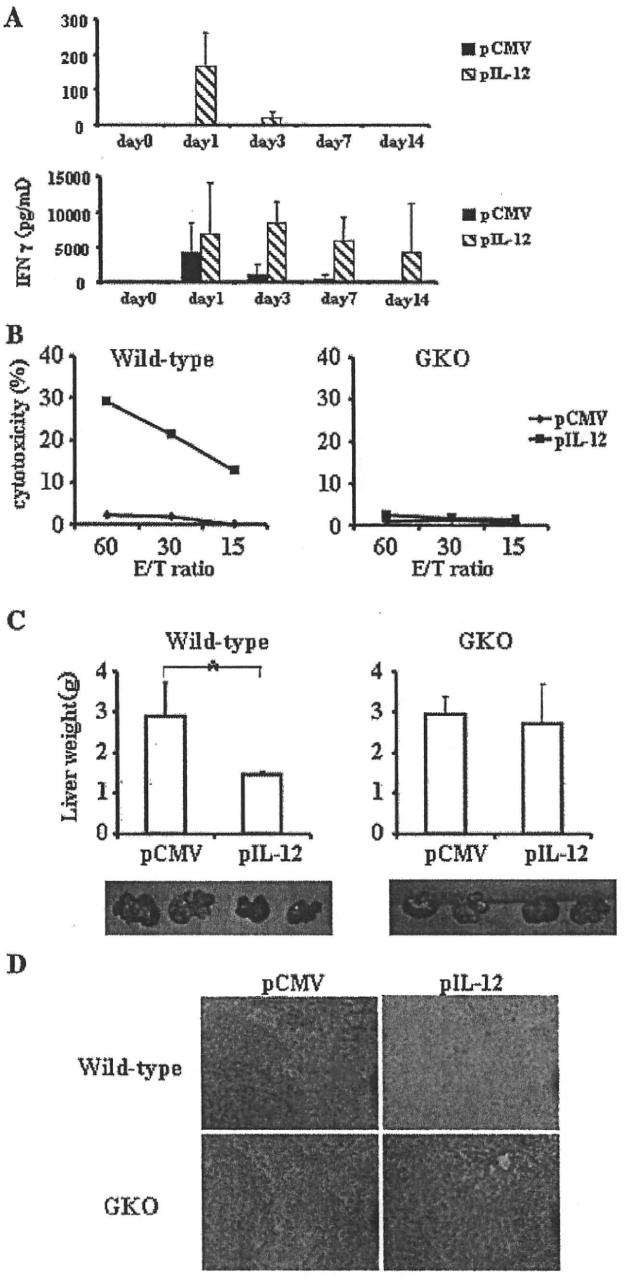

Fig. 1 Effects of hydrodynamic injection of IL-12-encoding plasmid. **a** Wild-type mice were hydrodynamically injected with either pCMV-IL-12 (*hatched bars*) or pCMV (*closed bars*) and bled at the indicated time points to measure the levels of serum IL-12 and IFNγ. Results are indicated as mean and SD ($n = 6$/group). **b** NK-cell activation after IL-12 administration. Hepatic mononuclear cells were isolated from wild-type mice (*left*) or GKO mice (*right*) which had been injected with pCMV-IL-12 (*closed squares*) or pCMV (*closed diamonds*) 4 days earlier. Yac1 lytic ability was measured by a standard ^{51}Cr-release assay at the indicated effector and target ratios (E/T ratio). All experiments were performed at least 3 times and representative data are shown. **c** and **d** Anti-metastatic effects of IL-12 therapy. Wild-type mice (*left*) or GKO mice (*right*) were intrasplenically injected with CT-26 cells and, 2 days later, hydrodynamically injected with either pCMV-IL-12 or pCMV. At 14 days after the plasmid injection, the mice were killed to examine liver tumor development. **c** Data are indicated as mean and SD of the liver weight at the top ($n = 6$/group) and a representative picture of the liver in each group is shown at the bottom. *$p < 0.001$. **d** Representative histology of liver sections

with those from naive mice or pCMV-injected mice. The levels of IFNγ production were highest in NK cells among those cells. Even at a later time point, 7 days after plasmid injection, NK cells were found to produce the highest levels of IFNγ (data not shown).

IL-12-induced STAT4 signaling and IFNγ production increased in NK cells

IL-12 activates Janus kinases Tyk2 and Jak2, STAT4 as well as other STATs. To examine the activation of STAT1 and STAT4, we isolated splenocytes from wild-type mice and GKO mice and stimulated them with IL-12 and/or IFNγ in the presence or absence of anti-IFNγ Ab (Fig. 3a). IL-12 led to phosphorylation of both STAT1 and STAT4 in wild-type splenocytes. In contrast, the same treatment led to phosphorylation of STAT4, but not of STAT1, in GKO splenocytes. Addition of IFNγ restored STAT1 phosphorylation in GKO splenocytes. Furthermore, adding anti-IFNγ inhibited STAT1 phosphorylation in wild-type cells. These findings demonstrated that phosphorylation of STAT4 is a direct effect of IL-12 but phosphorylation of STAT1 is indirect, via an autocrine or paracrine IFNγ-dependent manner.

To examine STAT1 and STAT4 activation and IFNγ production in NK cells and non-NK cells, we prepared whole mononuclear cells as well as NK and non-NK populations from wild-type spleens and stimulated the cells with IL-12 (Fig. 3b). NK cells expressed higher levels of STAT4 than non-NK cells. Upon IL-12 treatment, STAT4 was rapidly phosphorylated in NK cells, but to a lesser extent in non-NK cells. In contrast, NK cells expressed lesser levels of STAT1 than non-NK cells. STAT1 was similarly phosphorylated in NK cells and non-NK cells upon IL-12 treatment. Both NK cells and non-NK cells produced significant levels of IFNγ, but the levels were much higher in NK cells than non-NK cells (Fig. 3c). These results indicated that compared with non-NK cells, NK cells possessed higher levels of STAT4, a direct signaling molecule of IL-12, and produced higher levels of IFNγ than non-NK cells.

NK cells were sufficient for IL-12-mediated anti-tumor effects

The above observation indicated that NK cells are a predominant producer of IFNγ, which was critical for the IL-12-induced anti-tumor effects. To examine whether NK

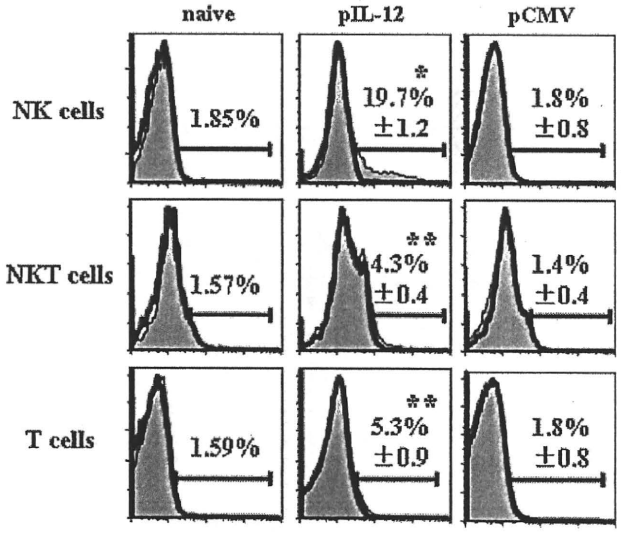

Fig. 2 IFNγ expression of mononuclear cells after IL-12 administration. Wild-type mice were injected with pCMV-IL-12 or pCMV, or were untreated (naive). Mononuclear cells were isolated from the liver 2 days after plasmid injection and stained with anti-TCRβ mAb, anti-DX5 mAb and anti-IFNγ mAb. *Closed histograms* show the IFNγ expression in the gated populations ($TCR\beta^-/DX5^+$ cells for NK cells, $TCR\beta^+/DX5^+$ cells for NKT cells and $TCR\beta^+/DX5^-$ cells for T cells). Isotype control stainings are shown by *open histograms*. Numbers in histograms represent averages ± SD of percentages of positive cells ($n = 3$ mice/group). $*p < 0.0001$ vs. mock in NK populations. $**p < 0.05$ vs. mock in each population

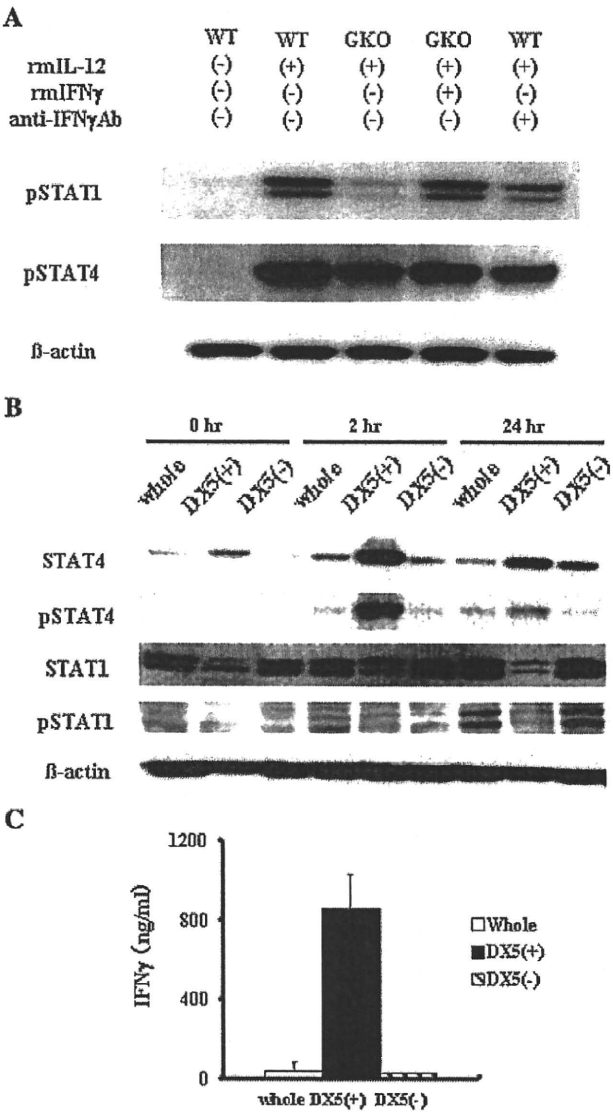

Fig. 3 STAT signaling and IFNγ production of mononuclear cells in vitro treated with IL-12. **a** STAT1 and STAT4 activation of splenocytes in vitro treated with IL-12. Splenocytes were isolated from wild-type mice or GKO mice and treated with or without recombinant IL-12 (20 ng/mL) in the presence or absence of recombinant IFNγ (500 ng/mL) or anti- IFNγ antibody (20 μg/mL) for 24 h. Cellular lysates were analyzed by Western blot for the expression of phospho-STAT1, phospho-STAT4 and β-actin. **b** and **c** STATs expression and signaling of NK cells and non-NK cells. Splenocytes were isolated from wild-type mice. Whole splenocytes were further purified into $DX5^+$ cells and $DX5^-$ cells. Each cell population was cultured with recombinant IL-12 (20 ng/mL) for the indicated times. **b** The cells were lysed to examine expression of whole STAT and phospho-STAT by Western blot. **c** The levels of IFNγ in the culture supernatant at 24 h were determined by ELISA. Data are expressed as mean and SD ($n = 3$)

cells are sufficient for the anti-metastatic effects of IL-12, we examined the anti-metastatic effect in Rag2 KO mice which lack T cells, B cells and NKT cells. pCMV-IL-12 injection enhanced the Yac1 lytic ability of hepatic mononuclear cells in Rag2 KO mice higher than in wild-type mice (Fig. 4a). To examine whether NK cells are sufficient for IL-12-mediated rejection of hepatic metastasis, we injected pCMV-IL-12 or pCMV into mice that had been intra-splenically injected with CT-26 cells 2 days earlier. Serum IFNγ levels of Rag2 KO mice were about 4 times higher than those of wild-type mice (Fig. 4b). pCMV-IL-12 completely suppressed hepatic metastasis in Rag2 KO mice (Fig. 4c).

Adoptive transfer of wild-type NK cells into GKO mice restored the anti-tumor effects of IL-12

Since NK cells were sufficient for producing IL-12-induced anti-tumor effects, we postulated that their production of IFNγ may play an important role in these effects. To test this, we performed adoptive transfer experiments with GKO mice. First, whole mononuclear cells isolated from the spleens of wild-type mice (2.0×10^8 cells) were adoptively transferred to GKO mice 1 day before plasmid injection. pCMV-IL-12 injection increased Yac1 lytic activity of hepatic mononuclear cells in the adoptively transferred group, but not in the untreated group (Fig. 5a). pCMV-IL-12 induced significant increase in serum IFNγ levels 4 days after plasmid injection in the adoptive transferred group, but not in the other groups (Fig. 5b). The

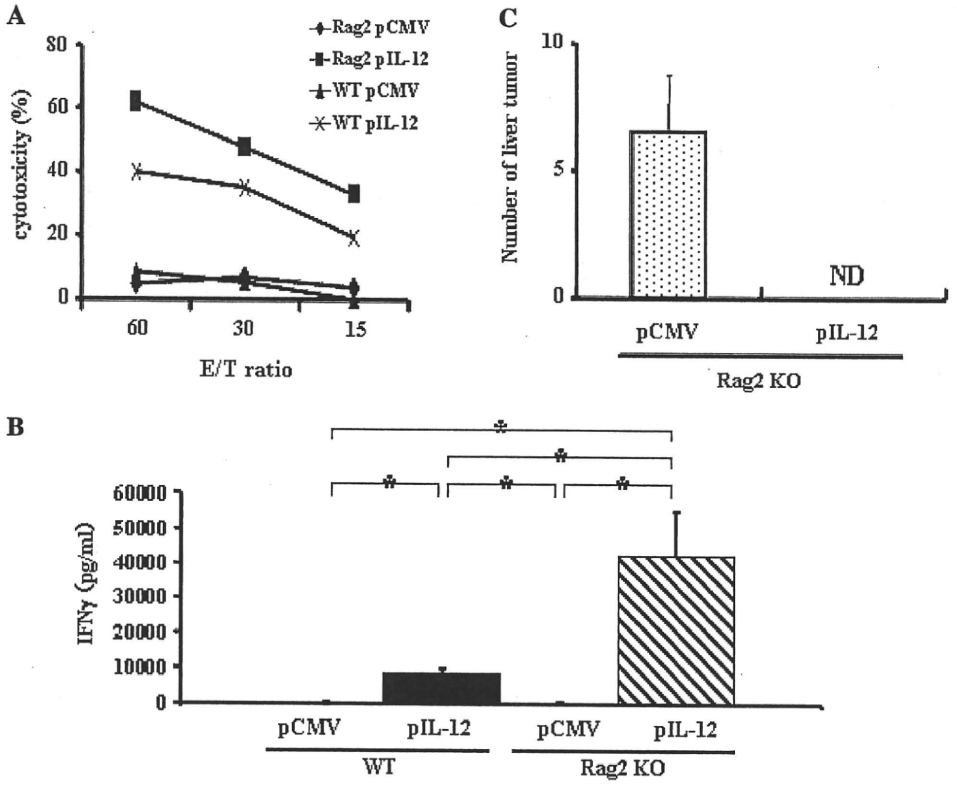

Fig. 4 Anti-tumor effects of IL-12 in Rag2 KO mice. Serum IFNγ levels and NK-cell activation. Wild-type or Rag2 KO mice were hydrodynamically injected with either pCMV-IL-12 or pCMV and killed at 4 days. **a** Yac1 lytic ability of hepatic mononuclear cells was determined by Cr releasing assay as the indicated effector and target ratios (E/T ratio). Experiments were done 2 times and representative data are shown. **b** The levels of serum IFNγ were determined by ELISA. Data are expressed as mean and SD ($n = 7$/group). $^*p < 0.0001$. **c** Anti-metastatic effect. Rag2 KO mice were intrasplenically injected with CT-26 cells and, 2 days later, hydrodynamically injected with either pCMV-IL-12 or pCMV. Fourteen days after plasmid injection, mice were killed to examine tumor development in the liver. The numbers of hepatic tumors in each group are expressed as mean and SD ($n = 7$/group). *ND* not detectable

anti-metastatic effect of IL-12 was restored in GKO mice when whole mononuclear cells from wild-type mice were adoptively transferred (Fig. 5c).

To evaluate the contribution of IFNγ production from each subset of mononuclear cells to the anti-metastatic effect of IL-12, we adoptively transferred the same number of whole mononuclear cells, NK cells or non-NK cells from wild-type mice (4.0×10^6 cells) 1 day before pCMV-IL-12 injection and analyzed liver tumor formation. Only in the NK-cell-transferred group, pCMV-IL-12 injection induced NK cytolytic ability in the liver and IFNγ elevation in serum 4 days after plasmid injection, but not in the other groups (Fig. 5d, e). No liver tumor formed in the NK-cell-transferred group. In contrast, livers in other groups had massive tumors, and the liver weights were significantly heavier than those in the NK-cell-transferred group (Fig. 5f). These results clearly demonstrated the strong impact of IFNγ produced from NK cells on IL-12-induced anti-tumor effects compared with that from non-NK cells.

Anti-tumor effects of IL-12 deteriorated slightly in mice depleted of NK cells

To examine the involvement of NK cells in the tumor deletion by IL-12 therapy, we induced depletion of NK cells by repeatedly injecting anti-asialoGM1 antibody. The cytolytic ability of NK cells was completely abolished in the anti-asialoGM1 antibody-injected group (Fig. 6a). Serum IFNγ induction by IL-12 in the NK depletion group was about half of that in the control immunoglobulin injected group (Fig. 6b). Unexpectedly, pCMV-IL-12 injection inhibited macroscopic liver metastasis of CT-26 cells in NK cell-depleted mice (Fig. 6c). However, a number of microscopic tumor regions were observed after IL-12 therapy in NK cell-depleted mice but not in control IgG-injected mice (Fig. 6d). This finding indicated that NK cells are required for a full-blown IL-12 anti-tumor effect, but IL-12's anti-tumor effect was still observed even if the NK cells were knocked down. To examine the underlying mechanisms of anti-tumor effect in NK cell-depleted mice,

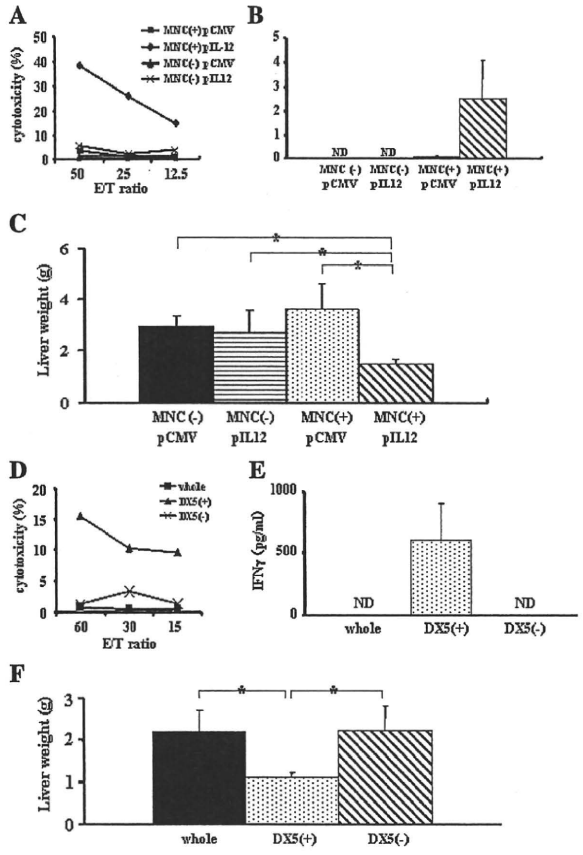

Fig. 5 Adoptive transfer of wild-type cells into GKO mice. Adoptive transfer of wild-type splenocytes restored anti-tumor effects of IL-12 in GKO mice. **a** GKO mice were intravenously injected with or without 2.0×10^8 splenocytes from wild-type mice and, 1 day later, hydrodynamically injected with either pCMV-IL-12 or pCMV. Mice were killed 4 days after plasmid injection. Yac1 lytic ability of hepatic mononuclear cells was expressed as the indicated effector and target ratios (E/T ratio). Experiments were done 3 times and representative data are shown. **b** and **c** GKO mice were intrasplenically injected with CT-26 cells and, 1 day later, intravenously injected with or without 2.0×10^8 splenocytes from wild-type mice. Two days after CT-26 injection, mice were hydrodynamically injected with either pCMV-IL-12 or pCMV. **b** The levels of serum IFNγ 4 days after plasmid injection are expressed as mean and SD ($n = 6$/group). **c** Fourteen days after plasmid injection, mice were killed to examine liver tumor development by measuring liver weight. The results are indicated as mean and SD ($n = 6$/group). *ND* not detectable. $^*p < 0.01$. Adoptive transfer of wild-type NK cells, but not non-NK cells, restored anti-tumor effects of IL-12 in GKO mice. **d** Wild-type splenocytes were purified into $DX5^+$ cells and $DX5^-$ cells. GKO mice were intravenously injected with 4.0×10^6 whole mononuclear cells or $DX5^+$ cells or $DX5^-$ cells and, 1 day later, hydrodynamically injected with either pCMV-IL-12 or pCMV. Mice were killed 4 days after hydrodynamic injection. Yac1 lytic ability of hepatic mononuclear cells is expressed as the indicated effector and target ratios (E/T ratio). Experiments were done 3 times and representative data are shown. **e** and **f** GKO mice were intrasplenically injected with CT-26 cells and, 1 day later, intravenously injected with whole mononuclear cells, $DX5^+$ cells or $DX5^-$ cells (4.0×10^6/mouse). Two days after CT-26 injection, mice were hydrodynamically injected with either pCMV-IL-12 or pCMV. **e** The levels of serum IFNγ are expressed as mean and SD ($n = 6$/group). **f** Fourteen days after plasmid injection, mice were killed to examine liver tumor development by measuring liver weight. The results are expressed as mean and SD ($n = 6$/group). *ND* not detectable. $^*p < 0.001$

serum levels of IP-10 and MIG, chemokines downstream of IFNγ, were measured after IL-12 therapy (Fig. 6e). pCMV-IL-12-injected mice showed significant increase in both levels compared with pCMV-injected mice. Significant increase after pCMV-IL-12 injection was also found in NK cell-depleted mice, but not in GKO mice. This result suggests that production of these chemokines was not completely suppressed in NK cell-depleted mice in our experimental condition. Immunohistochemical analysis revealed that tumoral accumulation of CD4-positive cells and CD8-positive cells was observed in pCMV-IL-12-injected mice but not in pCMV-injected mice. On the other hand, similar levels of CD31 expression were observed in tumors of pCMV-injected mice and pCMV-IL-12-injected mice (Fig. 6d). These results suggest that IL-12's anti-tumor effects might be mediated by T-cell accumulating in the tumor rather than anti-angiogenesis.

Discussion

IL-12 is recognized as a master regulator of adaptive type 1, cell-mediated immunity. One major action of IL-12 is its induction of other cytokines, particularly IFNγ. A large amount of evidence has indicated that IL-12 administration leads to IFNγ production from a variety of immune cells, such as T cells [16], B cells [17], NK cells [18] and NKT cells [22]. The relative impact of each immune cell as the source of IFNγ has been controversial. The present study highlighted NK cells as a most efficient producer of IFNγ that is critical for IL-12-induced anti-tumor effects.

Flow cytometric analysis revealed higher in vivo production of IFNγ of NK cells than that of other cell types. The levels of serum IFNγ were around fourfold higher in Rag2 KO mice which only possess NK cells than in wild-type mice. On the other hand, NK-cell depletion in wild-type mice led to twofold reduction of serum IFNγ levels. These data indicate substantial contribution of NK cells in IFNγ production in vivo. Previous research has demonstrated that the specific cellular effects of IL-12 are due mainly to activation of STAT4 [23, 24]. IL-12-induced STAT4 phosphorylation leads to the production of IFNγ [25]. In agreement with these reports, our in vitro analysis showed that, in contrast to STAT1, STAT4 was directly phosphorylated upon IL-12 stimulation, being independent of IFNγ. Of interest is the finding that NK cells express higher levels of STAT4 than non-NK cells, suggesting that NK cells possess an ideal expression profile of STATs for producing IFNγ upon IL-12 stimulation. Indeed, in vitro analysis revealed that NK cells, upon IL-12 exposure, displayed higher levels of IFNγ production as well as STAT4 phosphorylation than non-NK cells. These in vitro

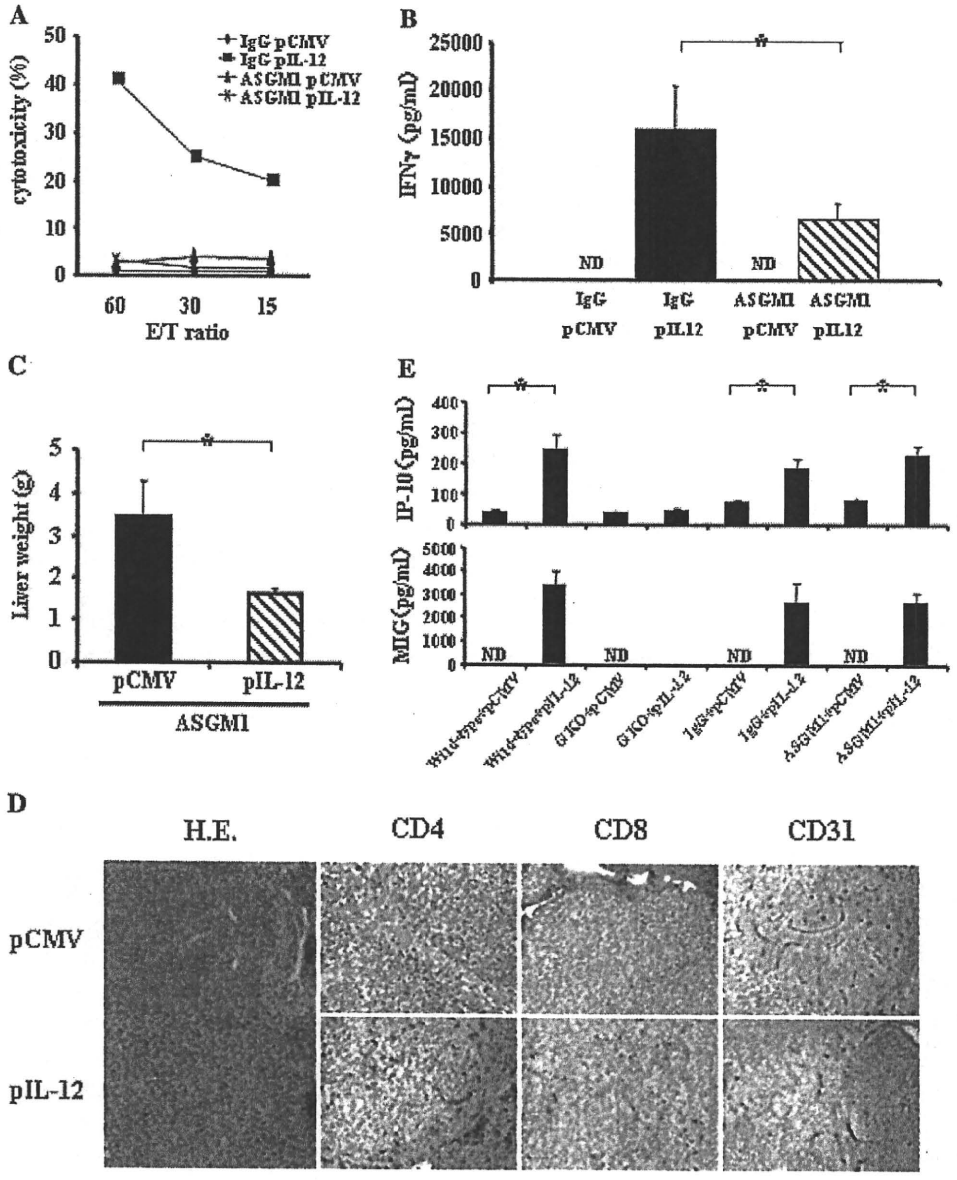

Fig. 6 Anti-tumor effects of IL-12 in NK-cell-depleted mice. Serum IFNγ levels and NK-cell activation. Wild-type mice were intraperitoneally injected with either anti-asialoGM1 antibody (ASGM1) or control IgG, and, 1 day later hydrodynamically injected with either pCMV-IL-12 or pCMV. Mice were killed 4 days after plasmid injection. **a** Yac1 lytic ability of hepatic mononuclear cells is expressed as the indicated effector and target ratios (E/T ratio). Experiments were done 2 times and representative data are shown. **b** The levels of serum IFNγ are expressed as mean and SD ($n = 6$/group). *ND* not detectable. $^*p < 0.005$. Anti-metastatic effects. Wild-type mice were intrasplenically injected with CT-26 cells and, 1 day later and then every 5 days, intraperitoneally injected with either anti-asialoGM1 antibody (ASGM1) or control IgG, and hydrodynamically injected with either pCMV-IL-12 or pCMV 2 days after CT-26 injection. Fourteen days after plasmid injection, mice were killed to examine liver tumor development by measuring liver weight. **c** The results are indicated as mean and SD ($n = 6$/group). $^*p < 0.001$. **d** Representative histology of liver sections analyzed by hematoxylin-eosin staining and immunohistochemistry of CD4, CD8 and CD31. **e** Serum levels of IP-10 and MIG. Wild-type or GKO mice were hydrodynamically injected with either pCMV-IL-12 or pCMV. Wild-type mice were intraperitoneally injected with either anti-asialoGM1 antibody (ASGM1) or control IgG, and 1 day later hydrodynamically injected with either pCMV-IL-12 or pCMV. Four days later, each mice were bled to measure the levels of serum IP-10 and MIG. Results are expressed as mean and SD ($n = 6$/group). *ND* not detectable. $^*p < 0.001$

data are consistent with the in vivo observation that NK cells are efficient producers of IFNγ during IL-12 therapy.

Many studies have demonstrated that IFNγ production is required for the anti-tumor effects of IL-12 [14, 26, 27]. In fact, we have demonstrated that deletion of IFNγ abolished NK cytotoxicity and the anti-metastatic effect of IL-12 therapy in the liver. A large amount of evidence supports the concept that a major action of IL-12 is to promote the differentiation of naïve CD4 + T cells into Th1 cells, which produce IFNγ. Previous research reported that CD4

T-cell depletion caused inhibition of anti-tumor effects. More recent studies have supported a critical role of IFNγ as a third signal for CD8 T-cell differentiation. There have been many reports focusing on IFNγ production from T cells induced by IL-12 for the anti-tumor effect of IL-12 [28]. Segal et al. performed an elegant study showing a critical role of T-cell production of IFNγ in the anti-tumor effect by adoptively transferring T cells into GKO mice in a subcutaneous tumor model [29]. However, apart from this study, little is known about the contribution of each immune cell as a producer of IFNγ in terms of an anti-tumor effect. In our model, T-cell mediated adaptive responses were not required for the anti-metastatic effect of IL-12. More importantly, the anti-metastatic effects of IL-12 were restored in GKO mice by an adoptive transfer of wild-type NK cells. The same number of non-NK cells could not provoke IL-12-induced anti-tumor effects in GKO mice. The present study demonstrated for the first time a potent effect of NK cells on producing IFNγ that was critical for anti-metastatic effect during IL-12 therapy.

Our study showed that the main IFNγ producer of IL-12 was NK cells. So we focused on NK cells which were activated by IL-12 in an IFNγ-dependent manner to examine the cellular mechanism of protection against hepatic metastasis. Many studies have shown the importance of each subset (NK- [12], NKT- [10] and T [9, 30] cells) for anti-tumor effects of IL-12. In the present study, NK cells were sufficient while T cells, B cells, NKT cells were dispensable for IL-12-mediated NK-cell activation and anti-metastatic effects as IL-12 therapy showed Yac1 lytic ability and antimetastatic effects in Rag2 KO mice. On the other hand, NK-cell depletion by a repeated injection of anti-aialoGM1 antibody protected wild-type mice from macroscopic liver metastasis, but did not from microscopic liver metastasis. Thus, although NK cells were required for a full-blown IL-12 anti-tumor effect, other anti-tumor pathways are activated by IL-12 in the absence of NK cells. Serum levels of IP-10 and MIG suggest that production of these chemokines downstream of IFNγ was not suppressed in NK-cell-depleted mice in our experimental condition. When compared with the experiment on GKO mice, accumulation of CD4-positive cells and CD8-positive cells were more evident in NK-cell-depleted mice than in GKO mice (Supplementary Figure). On the other hand, there was no remarkable difference in the expression of CD31 between pCMV injection and pCMV-IL-12 injection. These results suggested that in NK-cell-depleted mice IL-12 may exert anti-tumor effect via T-cell accumulation rather than anti-angiogenesis.

Since the liver contains an abundance of immune cells (especially NK cells) [31], the cytokine-mediated activation of these cells may be a promising approach toward anti-tumor therapy in this organ [32]. IL-12 is a cytokine known to elicit a potent anti-tumor effect in mouse experimental models. However, clinical trials attempted to date were interrupted by fatal adverse effects. Systemic IL-12 therapy has been associated with dose-limiting toxicity [33]. IL-12 induces activation of the pro-inflammatory pathway which causes the complications of high dose cytokine, independent of the action of IFNγ [34]. On the other hand, the levels of immunosuppressive cytokine, for example, TGF-β1 or IL-10 were significantly higher in patients with hepatocellular cancer and colon cancer [35–38]. In particular, TGF-β1 in serum can limit NK-cell IFNγ production [39]. Thus, in patients with advanced disease, IL-12 may not be able to exert its potent anti-tumor immune-effects because IFNγ, which is an important mediator of the IL-12-induced immune response, is less effective in a tumor environment. In the present study, we demonstrated that NK-cell IFNγ production induced by IL-12 was sufficient for the anti-metastatic effect of IL-12 in the liver. Thus, a strategy of efficiently producing IFNγ from NK cells may be important for avoiding toxicity of IL-12 therapy.

IL-12 gene therapy has an advantage to allow local production of the cytokine at the tumor sites with low serum concentration. Studies demonstrated that intratumoral administration of adenovirus encoding IL-12 to animals with different types of carcinoma caused complete tumor eradication and increased long-term survival [40, 41]. Moreover, injection of IL-12-encoding adenovirus in one nodule of liver tumor resulted in regression of distant nodules in the liver [41]. However, in a clinical trial anti-tumor activity of IL-12-encoding adenovirus was only observed in the injected tumor sites, but not in distant tumors [42]. The present study shed light on hydrodynamic transfection of hepatocytes as a promising strategy to eradicate disseminated tumors from whole liver.

In summary, NK cells are not just an effector for innate immunity but a mediator producing IFNγ that is critical for the IL-12 anti-tumor effects. Extremely higher expression of STAT4 may be a basis for efficient production of IFNγ from NK cells.

Acknowledgments We thank Dr. Morihiro Watanabe (Laboratory of Experimental Immunology, Division of Basic Sciences, National Cancer Institute-Frederick Cancer Research and Development Center) for providing the pCMV-IL-12 plasmid, Dr. Yoichiro Iwakura (University of Tokyo, Institute of Medical Science) for providing GKO mice.

References

1. Kobayashi M, Fitz L, Ryan M, Hewick RM, Clark SC, Chan S, Loudon R, Sherman F, Perussia B, Trinchieri G (1989) Identification and purification of natural killer cell stimulatory factor

(NKSF), a cytokine with multiple biologic effects on human lymphocytes. J Exp Med 170(3):827–845
2. Stern AS, Podlaski FJ, Hulmes JD, Pan YC, Quinn PM, Wolitzky AG, Familletti PC, Stremlo DL, Truitt T, Chizzonite R, Gately MK (1990) Purification to homogeneity and partial characterization of cytotoxic lymphocyte maturation factor from human B-lymphoblastoid cells. Proc Natl Acad Sci USA 87(17):6808–6812
3. Watford WT, Moriguchi M, Morinobu A, O'Shea JJ (2003) The biology of IL-12: coordinating innate and adaptive immune responses. Cytokine Growth Factor Rev 14(5):361–368
4. Trinchieri G (2003) Interleukin-12 and the regulation of innate resistance and adaptive immunity. Nat Rev Immunol 3(2):133–146
5. Colombo MP, Trinchieri G (2002) Interleukin-12 in anti-tumor immunity and immunotherapy. Cytokine Growth Factor Rev 13(2):155–168
6. Del Vecchio M, Bajetta E, Canova S, Lotze MT, Wesa A, Parmiani G, Anichini A (2007) Interleukin-12: biological properties and clinical application. Clin Cancer Res 13(16):4677–4685
7. Wigginton JM, Gruys E, Geiselhart L, Subleski J, Komschlies KL, Park JW, Wiltrout TA, Nagashima K, Back TC, Wiltrout RH (2001) IFN-gamma and Fas/FasL are required for the antitumor and antiangiogenic effects of IL-12/pulse IL-2 therapy. J Clin Invest 108(1):51–62
8. Lee JC, Kim DC, Gee MS, Saunders HM, Sehgal CM, Feldman MD, Ross SR, Lee WM (2002) Interleukin-12 inhibits angiogenesis and growth of transplanted but not in situ mouse mammary tumor virus-induced mammary carcinomas. Cancer Res 62(3):747–755
9. Brunda MJ, Luistro L, Warrier RR, Wright RB, Hubbard BR, Murphy M, Wolf SF, Gately MK (1993) Antitumor and antimetastatic activity of interleukin 12 against murine tumors. J Exp Med 178(4):1223–1230
10. Cui J, Shin T, Kawano T, Sato H, Kondo E, Toura I, Kaneko Y, Koseki H, Kanno M, Taniguchi M (1997) Requirement for Valpha14 NKT cells in IL-12-mediated rejection of tumors. Science 278(5343):1623–1626
11. Zilocchi C, Stoppacciaro A, Chiodoni C, Parenza M, Terrazzini N, Colombo MP (1998) Interferon gamma-independent rejection of interleukin 12-transduced carcinoma cells requires CD4 + T cells and Granulocyte/Macrophage colony-stimulating factor. J Exp Med 188(1):133–143
12. Kodama T, Takeda K, Shimozato O, Hayakawa Y, Atsuta M, Kobayashi K, Ito M, Yagita H, Okumura K (1999) Perforin-dependent NK cell cytotoxicity is sufficient for anti-metastatic effect of IL-12. Eur J Immunol 29(4):1390–1396
13. Takeda K, Hayakawa Y, Atsuta M, Hong S, Van Kaer L, Kobayashi K, Ito M, Yagita H, Okumura K (2000) Relative contribution of NK and NKT cells to the anti-metastatic activities of IL-12. Int Immunol 12(6):909–914
14. Ogawa M, Yu WG, Umehara K, Iwasaki M, Wijesuriya R, Tsujimura T, Kubo T, Fujiwara H, Hamaoka T (1998) Multiple roles of interferon-gamma in the mediation of interleukin 12-induced tumor regression. Cancer Res 58(11):2426–2432
15. Subleski JJ, Hall VL, Back TC, Ortaldo JR, Wiltrout RH (2006) Enhanced antitumor response by divergent modulation of natural killer and natural killer T cells in the liver. Cancer Res 66(22):11005–11012
16. Kubin M, Kamoun M, Trinchieri G (1994) Interleukin 12 synergizes with B7/CD28 interaction in inducing efficient proliferation and cytokine production of human T cells. J Exp Med 180(1):211–222
17. Yoshimoto T, Okamura H, Tagawa YI, Iwakura Y, Nakanishi K (1997) Interleukin 18 together with interleukin 12 inhibits IgE production by induction of interferon-gamma production from activated B cells. Proc Natl Acad Sci USA 94(8):3948–3953
18. Lauwerys BR, Renauld JC, Houssiau FA (1999) Synergistic proliferation and activation of natural killer cells by interleukin 12 and interleukin 18. Cytokine 11(11):822–830
19. Takehara T, Uemura A, Tatsumi T, Suzuki T, Kimura R, Shiotani A, Ohkawa K, Kanto T, Hiramatsu N, Hayashi N (2007) Natural killer cell-mediated ablation of metastatic liver tumors by hydrodynamic injection of IFNalpha gene to mice. Int J Cancer 120(6):1252–1260
20. Watanabe M, Fenton RG, Wigginton JM, McCormick KL, Volker KM, Fogler WE, Roessler PG, Wiltrout RH (1999) Intradermal delivery of IL-12 naked DNA induces systemic NK cell activation and Th1 response in vivo that is independent of endogenous IL-12 production. J Immunol 163(4):1943–1950
21. Takehara T, Suzuki T, Ohkawa K, Hosui A, Jinushi M, Miyagi T, Tatsumi T, Kanazawa Y, Hayashi N (2006) Viral covalently closed circular DNA in a non-transgenic mouse model for chronic hepatitis B virus replication. J Hepatol 44(2):267–274
22. Shin T, Nakayama T, Akutsu Y, Motohashi S, Shibata Y, Harada M, Kamada N, Shimizu C, Shimizu E, Saito T, Ochiai T, Taniguchi M (2001) Inhibition of tumor metastasis by adoptive transfer of IL-12-activated Valpha14 NKT cells. Int J Cancer 91(4):523–528
23. Thierfelder WE, van Deursen JM, Yamamoto K, Tripp RA, Sarawar SR, Carson RT, Sangster MY, Vignali DA, Doherty PC, Grosveld GC, Ihle JN (1996) Requirement for Stat4 in interleukin-12-mediated responses of natural killer and T cells. Nature 382(6587):171–174
24. Kaplan MH, Sun YL, Hoey T, Grusby MJ (1996) Impaired IL-12 responses and enhanced development of Th2 cells in Stat4-deficient mice. Nature 382(6587):174–177
25. Morinobu A, Gadina M, Strober W, Visconti R, Fornace A, Montagna C, Feldman GM, Nishikomori R, O'Shea JJ (2002) STAT4 serine phosphorylation is critical for IL-12-induced IFN-gamma production but not for cell proliferation. Proc Natl Acad Sci USA 99(19):12281–12286
26. Comes A, Di Carlo E, Musiani P, Rósso O, Meazza R, Chiodoni C, Colombo MP, Ferrini S (2002) IFN-gamma-independent synergistic effects of IL-12 and IL-15 induce anti-tumor immune responses in syngeneic mice. Eur J Immunol 32(7):1914–1923
27. Hafner M, Falk W, Echtenacher B, Mannel DN (1999) Interleukin-12 activates NK cells for IFN-gamma-dependent and NKT cells for IFN-gamma-independent antimetastatic activity. Eur Cytokine Netw 10(4):541–548
28. Komita H, Homma S, Saotome H, Zeniya M, Ohno T, Toda G (2006) Interferon-gamma produced by interleukin-12-activated tumor infiltrating CD8 + T cells directly induces apoptosis of mouse hepatocellular carcinoma. J Hepatol 45(5):662–672
29. Segal JG, Lee NC, Tsung YL, Norton JA, Tsung K (2002) The role of IFN-gamma in rejection of established tumors by IL-12: source of production and target. Cancer Res 62(16):4696–4703
30. Nastala CL, Edington HD, McKinney TG, Tahara H, Nalesnik MA, Brunda MJ, Gately MK, Wolf SF, Schreiber RD, Storkus WJ, Lotze MT (1994) Recombinant IL-12 administration induces tumor regression in association with IFN-gamma production. J Immunol 153(4):1697–1706
31. Doherty DG, O'Farrelly C (2000) Innate and adaptive lymphoid cells in the human liver. Immunol Rev 174:5–20
32. Seki S, Habu Y, Kawamura T, Takeda K, Dobashi H, Ohkawa T, Hiraide H (2000) The liver as a crucial organ in the first line of host defense: the roles of Kupffer cells, natural killer (NK) cells and NK1.1 Ag + T cells in T helper 1 immune responses. Immunol Rev 174:35–46
33. Car BD, Eng VM, Lipman JM, Anderson TD (1999) The toxicology of interleukin-12: a review. Toxicol Pathol 27(1):58–63
34. Biber JL, Jabbour S, Parihar R, Dierksheide J, Hu Y, Baumann H, Bouchard P, Caligiuri MA, Carson W (2002) Administration of

two macrophage-derived interferon-gamma-inducing factors (IL-12 and IL-15) induces a lethal systemic inflammatory response in mice that is dependent on natural killer cells but does not require interferon-gamma. Cell Immunol 216(1–2):31–42
35. Tsushima H, Ito N, Tamura S, Matsuda Y, Inada M, Yabuuchi I, Imai Y, Nagashima R, Misawa H, Takeda H, Matsuzawa Y, Kawata S (2001) Circulating transforming growth factor beta 1 as a predictor of liver metastasis after resection in colorectal cancer. Clin Cancer Res 7(5):1258–1262
36. Okumoto K, Hattori E, Tamura K, Kiso S, Watanabe H, Saito K, Saito T, Togashi H, Kawata S (2004) Possible contribution of circulating transforming growth factor-beta1 to immunity and prognosis in unresectable hepatocellular carcinoma. Liver Int 24(1):21–28
37. Chau GY, Wu CW, Lui WY, Chang TJ, Kao HL, Wu LH, King KL, Loong CC, Hsia CY, Chi CW (2000) Serum interleukin-10 but not interleukin-6 is related to clinical outcome in patients with resectable hepatocellular carcinoma. Ann Surg 231(4):552–558
38. Galizia G, Lieto E, De Vita F, Romano C, Orditura M, Castellano P, Imperatore V, Infusino S, Catalano G, Pignatelli C (2002) Circulating levels of interleukin-10 and interleukin-6 in gastric and colon cancer patients before and after surgery: relationship with radicality and outcome. J Interferon Cytokine Res 22(4):473–482
39. Meadows SK, Eriksson M, Barber A, Sentman CL (2006) Human NK cell IFN-gamma production is regulated by endogenous TGF-beta. Int Immunopharmacol 6(6):1020–1028
40. Caruso M, Pham-Nguyen K, Kwong YL, Xu B, Kosai KI, Finegold M, Woo SL, Chen SH (1996) Adenovirus-mediated interleukin-12 gene therapy for metastatic colon carcinoma. Proc Natl Acad Sci USA 93(21):11302–11306
41. Barajas M, Mazzolini G, Genove G, Bilbao R, Narvaiza I, Schmitz V, Sangro B, Melero I, Qian C, Prieto J (2001) Gene therapy of orthotopic hepatocellular carcinoma in rats using adenovirus coding for interleukin 12. Hepatology 33(1):52–61
42. Sangro B, Mazzolini G, Ruiz J, Herraiz M, Quiroga J, Herrero I, Benito A, Larrache J, Pueyo J, Subtil JC, Olague C, Sola J et al (2004) Phase I trial of intratumoral injection of an adenovirus encoding interleukin-12 for advanced digestive tumors. J Clin Oncol 22(8):1389–1397

J Gastroenterol (2010) 45:1247–1254
DOI 10.1007/s00535-010-0272-y

ORIGINAL ARTICLE—LIVER, PANCREAS, AND BILIARY TRACT

Absence of invariant natural killer T cells deteriorates liver inflammation and fibrosis in mice fed high-fat diet

Takuya Miyagi · Tetsuo Takehara · Akio Uemura · Kumiko Nishio · Satoshi Shimizu · Takahiro Kodama · Hayato Hikita · Wei Li · Akira Sasakawa · Tomohide Tatsumi · Kazuyoshi Ohkawa · Tatsuya Kanto · Naoki Hiramatsu · Norio Hayashi

Received: 28 November 2009 / Accepted: 31 May 2010 / Published online: 2 July 2010

Abstract
Background Invariant natural killer T (iNKT) cells have been suggested to play critical roles in a wide range of immune responses by acting in a proinflammatory or anti-inflammatory manner. Nonalcoholic steatohepatitis (NASH) is a chronic liver disease progressing to advanced cirrhosis and hepatocellular carcinoma. Despite the abundance of iNKT cells in the liver, their role in the pathogenesis of NASH remains obscure. Here, we investigated their role in the development of diet-induced steatosis/steatohepatitis.
Methods We used BALB/c wild-type mice and Jα18-deficient (KO) mice lacking iNKT cells fed either a normal diet or a high-fat diet (HFD). The liver and blood were collected from these mice to examine liver inflammation, steatosis, and fibrosis at the indicated time points.
Results KO mice fed the HFD, compared with control mice fed the HFD, exhibited a clearly higher serum alanine aminotransferase level and a greater number of hepatic inflammatory foci, although there was no significant difference in hepatic lipid retention between these groups of mice. The HFD enhanced hepatic messenger RNA expression of inflammatory cytokines and chemokines in KO but not in control mice. The HFD also increased the proportion of hepatic CD4 T cells and CD8 T cells that composed hepatic inflammatory foci in KO mice, but not in the controls. Prolonged feeding with the HFD augmented liver fibrosis in KO but not in control mice.
Conclusions These findings indicate that iNKT cells play a protective role against liver inflammation progressing to fibrosis, but not against steatosis, enhanced by dietary excess fat, suggesting a key role of these cells in NASH pathogenesis.

Keywords iNKT cells · Nonalcoholic fatty liver disease · Nonalcoholic steatohepatitis · Cytokine · Chemokine

Abbreviations

NAFLD	Nonalcoholic fatty liver disease
NASH	Nonalcoholic steatohepatitis
iNKT	Invariant natural killer T
NK	Natural killer
TCR	T cell receptor
Th	T helper
IFN	Interferon
IL	Interleukin
WT	Wild type
ND	Normal diet
HFD	High-fat diet
KO	Jα18-deficient
ALT	Alanine aminotransferase
RT-PCR	Reverse transcription polymerase chain reaction
H&E	Hematoxylin–eosin
SEM	Standard error of the mean
TNF	Tumor necrosis factor
CCL	Chemokine (C–C motif) ligand
CXCL	Chemokine (C–X–C motif) ligand

T. Miyagi · T. Takehara · A. Uemura · K. Nishio · S. Shimizu · T. Kodama · H. Hikita · W. Li · A. Sasakawa · T. Tatsumi · K. Ohkawa · T. Kanto · N. Hiramatsu · N. Hayashi (✉)
Department of Gastroenterology and Hepatology,
Osaka University Graduate School of Medicine,
2-2 Yamada-oka, Suita, Osaka 565-0871, Japan
e-mail: hayashin@gh.med.osaka-u.ac.jp

Introduction

Nonalcoholic fatty liver disease (NAFLD) is a spectrum of liver disorders ranging from nonalcoholic steatosis to nonalcoholic steatohepatitis (NASH), which can develop to progressive disease including advanced liver fibrosis and hepatocellular carcinoma [1, 2]. Prolonged overnutrition causes accumulation of free fatty acid and triglycerides within the liver, which is referred to as steatosis. Simple steatosis leads to a predisposition for steatohepatitis, which exhibits inflammatory cell accumulation and fibrosis in the liver in addition to the steatosis [1, 2]. To transform from steatosis to steatohepatitis, several key biological responses such as oxidative stress, mitochondrial dysfunction, endoplasmic reticulum stress, and abnormal cytokine properties have been reported to be required [1–4]. However, the immunological aspect, in particular, that is involved in the development of steatosis/steatohepatitis remains to be fully elucidated.

Invariant natural killer T (iNKT) cells are characterized by the expression of surface markers of natural killer (NK) cells together with a single invariant T cell receptor (TCR) encoded by Vα14-Jα18 in mice and Vα24-Jα18 in humans [5]. These cells are included within the population of T cells expressing NK cell markers, also known as NKT cells [5, 6]. iNKT cells recognize glycolipid antigens presented in association with the major histocompatibility complex class Ib molecule CD1d [5], which is expressed on a variety of cells including dendritic cells, B cells, and stellate cells, as well as hepatocytes in the liver [5, 7, 8]. Following the recognition of antigens via TCR, iNKT cells have the ability to produce the T-helper (Th) 1 cytokine, interferon (IFN)-γ, and the Th2 cytokines, interleukin (IL)-4, -5, and -13, modulating subsequent immune responses [5, 6, 9]. These cells have been shown to play a proinflammatory role in some immune responses and an anti-inflammatory role in other immune responses [5, 6, 9]. iNKT cells most frequently reside in the liver in mice [10, 11]. Although humans appear to have proportionally fewer iNKT cells than mice, human iNKT cells also preferentially reside in the liver [12, 13]. Several lines of evidence indicate that the number of NKT cells is dysregulated in the development of NAFLD. Hepatic iNKT cells or NK1.1+ CD3+/TCRβ+ NKT cells, for instance, have been reported to decrease with the development of steatosis in wild-type (WT) as well as leptin-deficient ob/ob mice [14–17]. A reduced level of peripheral Vα24+ NKT cells has been associated with human NAFLD [18]. On the other hand, CD56+ CD3+ NKT cells have been recently reported to be increased in the livers of patients with NAFLD [19]. Also, the adoptive transfer of NK1.1+ CD3+ NKT cells has been shown to alleviate hepatic steatosis in ob/ob mice [20]. However, the precise role of NKT cells in the pathogenesis of NAFLD has not been investigated in the presence of a deficiency of these cells.

In the present study, we used iNKT cell-deficient as well as WT mice fed either a normal diet (ND) or a high-fat diet (HFD), and examined the role of these cells in the development of HFD-induced steatosis/steatohepatitis. We found that the lack of iNKT cells, together with the HFD, led to liver inflammation, which was characterized by the enhanced gene expression of inflammatory cytokines and chemokines and by T cell accumulation. We also found that prolonged liver inflammation in the absence of iNKT cells developed to liver fibrosis which was strongly enhanced by the HFD. This study delineated an immunoregulatory function of iNKT cells and their key role against liver inflammation progressing to fibrosis exacerbated by an HFD, which might represent a clinical aspect of human progressive NAFLD.

Materials and methods

Animals and animal care

Specific pathogen-free BALB/c WT mice were purchased from CLEA Japan (Tokyo, Japan) as needed. Breeding pairs of BALB/c Jα18-deficient (KO) mice [21, 22] were provided by Drs. Masaru Taniguchi and Ken-ichiro Seino (RIKEN, Yokohama, Japan). The KO mice were confirmed to have no iNKT cells by the use of mouse-CD1d tetramers loaded with α-galactosylceramide in the flow cytometry procedure described below (data not shown). These mice were kept in isolation facilities at the Institute of Experimental Animal Science, Osaka University. They were housed in groups of five in filter cages and were maintained in a temperature-controlled, specific-pathogen-free room on 12-h light and dark cycles with ad libitum access to water and diet as indicated.

Experimental protocol

Male mice used in the experiments were fed an irradiated HFD consisting of 56.7% of the calories from fat (HFD32; CLEA Japan) or an irradiated ND consisting of 14% of the calories from fat (CRF-1; Oriental Yeast, Osaka, Japan), starting from when the mice were 6–8 weeks old. In preliminary experiments, we monitored the body weight of the WT mice and KO mice fed the ND or HFD every 2 weeks after the initiation of feeding, because a gain of body weight usually parallels the level of hepatic steatosis as well as obesity. We did not observe a gain of body weight of more than 25% until 4 weeks after the initiation of feeding. In mice fed the HFD, the body weight gain reached a plateau around 14–16 weeks after the initiation

of feeding. These observations led us to set the time point for estimating liver steatosis and injury and inflammation or liver fibrosis during the course of feeding at week 5 or week 15, respectively. At the end of the indicated periods, the mice were weighed and anesthetized with pentobarbital sodium, and then their abdomens were opened. Following blood sampling via the inferior caval vein, the portal vein and inferior caval vein were cut to enable blood outflow and then the liver was removed, weighed, and processed for further analyses. All animal experimental protocols were approved by the Institute of Experimental Animal Science, Osaka University. To evaluate the levels of liver injury, serum alanine aminotransferase (ALT) activities were measured as previously described [23]. To determine the levels of steatosis, total lipids were extracted from the liver and then triglyceride content was measured as previously described [24].

Flow cytometric analysis

Liver mononuclear cell populations were prepared as previously described [11, 23]. Cell surface staining of the prepared cells was performed as described [11, 23], using the following antibodies or tetramers: fluorescein isothiocyanate-conjugated anti-CD49b (DX5), phycoerythrin-conjugated anti-CD4 (H129.19), peridinin chlorophyll protein-conjugated anti-CD8α (53-6.7), and allophycocyanin-conjugated anti-TCRβ (H57-597) monoclonal antibody, or fluorescein isothiocyanate-conjugated anti-TCRβ, phycoerythrin-conjugated anti-CD4, peridinin chlorophyll protein-conjugated anti-CD45R/B220 (RA3-6B2) monoclonal antibody, and allophycocyanin-conjugated mouse-CD1d tetramers loaded with α-galactosylceramide. All antibodies were purchased from BD Biosciences (San Jose, CA, USA). Mouse CD1d tetramer was obtained from Proimmune (Oxford, UK) and the loading with α-galactosylceramide was performed following the manufacturer's protocol. The stained cells were analyzed with a FACScan (Becton Dickinson, Mountain View, CA, USA), and the data were processed using the CELLQuest program (Becton Dickinson). iNKT cells were detected on electronically gated CD45R/B220- TCRβ+ CD1d-tetramer-reactive cells.

RNA isolation and analysis

Total RNA was isolated from frozen liver tissues by using an RNeasy kit (QIAGEN, Hilden, Germany) following the manufacturer's protocol. Complementary DNA was synthesized from isolated RNA using SuperScript III and random hexamer (Invitrogen, Carlsbad, CA, USA). Real-time reverse transcription polymerase chain reaction (RT-PCR) analysis was performed using TaqMan Gene Expression Assays (Applied Biosystems, Foster City, CA, USA) normalized to beta-actin.

Histological evaluation

The removed liver was partly fixed in 10% formalin for staining with hematoxylin–eosin (H&E), Sirius-Red, or Oil-red-O, or it was immediately embedded in Tissue-Tek OCT compound (Sakura Finetechnical, Tokyo, Japan) and frozen in liquid nitrogen for immunohistochemical staining. Sirius-Red staining was performed to assess liver fibrosis, which was quantified by the extent of the area, using image-analysis software, WinROOF (Mitani, Fukui, Japan). Intracellular lipid was stained with Oil-red-O. To evaluate the infiltration of CD4+ cells or CD8+ cells into the liver, acetone-fixed fresh-frozen tissue sections were immunostained with anti-mouse CD4 (H129.19) or anti-mouse CD8α (53-6.7) monoclonal antibody, respectively, using a VECTASTAIN ABC kit (Vector Laboratories, Burlingame, CA, USA) following the manufacturer's protocol. The sections were developed with diaminobenzidine (DAB) substrate (Vector Laboratories) and then counterstained with hematoxylin. Antibody against CD4 or CD8 was purchased from BD Biosciences.

Statistical analysis

The statistical significance of differences between two groups was determined by applying the Mann–Whitney *U*-test. Statistical significance was defined as $P < 0.05$. All data are shown as mean ± standard error of the mean (SEM).

Results

Lipid accumulation in the liver induced by the HFD was independent of the presence or absence of iNKT cells

To investigate the role of iNKT cells in the development of diet-induced steatosis/steatohepatitis, we fed the ND or HFD to WT and KO mice for 5 weeks. The HFD increased the body weight by around 30% at week 5 in both WT and KO mice, while the ND increased it by around 14% (HFD-fed WT mice 31.6 ± 2.4%, HFD-fed KO mice 29.7 ± 5.6%, ND-fed WT mice 15.5 ± 0.6%, ND-fed KO mice 13.5 ± 1.1%; $n = 5$). The weight gains with the HFD or ND were not significantly different between WT and KO mice. Evaluation of the liver weight at week 5 showed that the HFD-fed WT or KO mice possessed significantly heavier livers than the ND-fed WT or KO mice, respectively, without any significant differences between the WT and KO mice (HFD-fed WT mice 1.95 ± 0.06 g, HFD-fed

KO mice 1.89 ± 0.07 g, ND-fed WT mice 1.52 ± 0.04 g, ND-fed KO mice 1.50 ± 0.06 g; $n = 5$).

We next performed Oil-red-O staining of liver sections from the mice to examine whether the absence of iNKT cells would affect the HFD-induced lipid accumulation in the liver. The staining showed that the HFD, compared with the ND, induced marked lipid retention in hepatocytes in both WT and KO mice (Fig. 1a). Evaluation of the liver triglyceride level demonstrated that the HFD, compared with the ND, clearly induced triglyceride accumulation in the livers of both WT and KO mice, without a significant difference between these groups of mice (Fig. 1b).

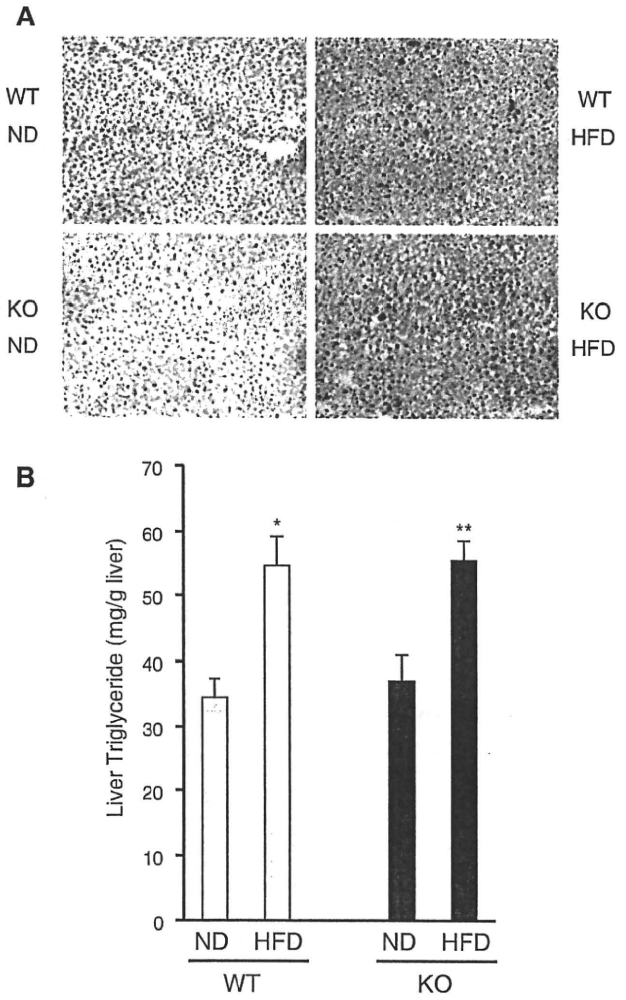

Fig. 1 Lipid accumulation in the liver induced by high-fat diet (*HFD*). Livers were obtained from BALB/c wild-type (*WT*) and BALB/c Jα18-deficient (*KO*) mice fed either a normal diet (*ND*) or an HFD for 5 weeks. **a** Lipid accumulation in liver sections was visualized by Oil-red-O staining. Representative images are shown (×200). **b** Hepatic triglyceride levels were quantified. Data shown are means ± SEM from five mice in each group. Data are representative of more than four independent experiments. $*P < 0.05$ versus WT fed ND. $**P < 0.05$ versus KO fed ND

Collectively, these results suggested that the absence of iNKT cells did not affect the level of HFD-induced steatosis.

HFD augmented liver injury and inflammation in the absence of iNKT cells

To examine the levels of liver injury, we measured ALT activity in serum from WT and KO mice fed the ND or HFD at week 5 after the start of being fed the diets. The serum ALT level in the HFD-fed WT mice (35.8 ± 1.98 IU/l) was significantly higher than that in the ND-fed WT mice (25.2 ± 0.66 IU/l) (Fig. 2a). The serum ALT level in the HFD-fed KO mice (174.8 ± 61.2 IU/l) was also significantly higher than that in the ND-fed KO mice (36.4 ± 7.48 IU/l). It was also higher than that in the HFD-fed KO mice at week 2 (83.3 ± 16.5 IU/l). Of note is the finding that the magnitude of the increase in ALT level at week 5 was clearly much higher in KO (4.9-fold) than in

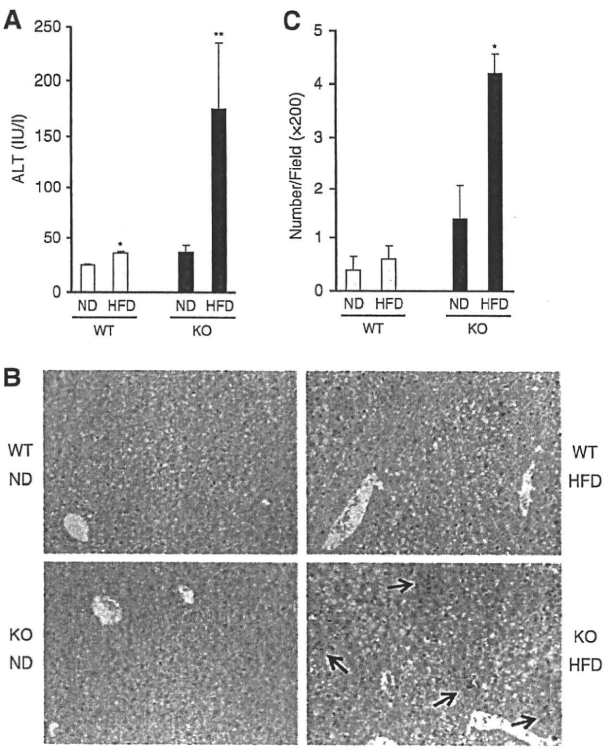

Fig. 2 Liver injury and inflammation exacerbated by HFD in the absence of invariant natural killer T (*iNKT*) cells. Serum and livers were obtained from wild-type (*WT*) and Jα18-deficient (*KO*) mice fed either a normal diet (*ND*) or a high-fat diet (*HFD*) for 5 weeks. **a** Serum alanine aminotransferase (*ALT*) levels were measured. $*P < 0.05$ versus WT fed ND. $**P < 0.05$ versus KO fed ND. **b** Liver tissues were stained with hematoxylin–eosin. Representative images are shown (×200). *Arrows* indicate the inflammatory foci. **c** The numbers of the foci were counted in five different fields per section. $*P < 0.05$ versus KO fed ND. All data shown are means ± SEM from five mice in each group. Data are representative of more than four independent experiments

WT mice (1.5-fold), even though the serum ALT level in the ND-fed KO mice was modestly higher than that in the ND-fed WT mice.

We next conducted histological analyses of liver sections from the mice. H&E staining revealed that the livers from KO mice fed the HFD possessed not only steatotic areas but also scattered inflammatory foci composed of gathering nonparenchymal cells (Fig. 2b). Although inflammatory foci were also observed in the livers from KO mice fed the ND, a larger number of foci could clearly be seen in KO mice fed the HFD than in KO mice fed the ND (Fig. 2c). In contrast, WT mice fed the HFD, as well as those given the ND, showed few inflammatory foci. Taken together, these results indicated that the HFD augmented liver inflammation in KO mice but not in WT mice.

The HFD enhanced hepatic inflammation-related gene expression in the absence of iNKT cells

To understand the underlying mechanisms of the hepatic inflammation induced by the HFD in the absence of iNKT cells, we first examined the levels of several cytokines and chemokines in the livers from mice at week 5 after they had been started on the diets. Real-time RT-PCR analyses revealed that the messenger RNA expression of tumor necrosis factor (TNF)-α, IFN-γ, IL-10, chemokine (C–C motif) ligand (CCL) 2 and 4, and chemokine (C–X–C motif) ligand (CXCL) 9 and 10 were remarkably upregulated by the HFD, compared with the ND, in KO but not in WT mice (Fig. 3), although these values in KO mice fed the ND were modestly higher than those in WT mice fed the ND. In contrast, the messenger RNA expression of IL-4, -5, and -13 did not show any detectable levels in the livers from both WT and KO mice fed either the ND or HFD.

The HFD altered the proportions of subpopulations in liver mononuclear cells from KO mice, but not in those from WT mice

We next examined the phenotype of mononuclear cells in livers from mice at week 5 of feeding. Flow cytometric analyses demonstrated that the proportion of CD4+ TCRβ+ CD4 T cells was lower in KO mice fed the ND than in WT mice fed the ND (Fig. 4a), which might have resulted from a lack of iNKT cells partly composed of CD4+ cells [5]. The proportion of CD49b+ TCRβ− NK cells or CD8+ TCRβ+ CD8 T cells was higher in KO mice fed the ND than in WT mice fed the ND. The HFD did not lead to any significant changes in the proportion of hepatic CD4 T, CD8 T, NK, or iNKT cells in WT mice. In contrast, the HFD induced significant increases in the proportion of hepatic CD4 T cells and CD8 T cells, but not of NK cells, in KO mice. We then examined the distribution of these cells

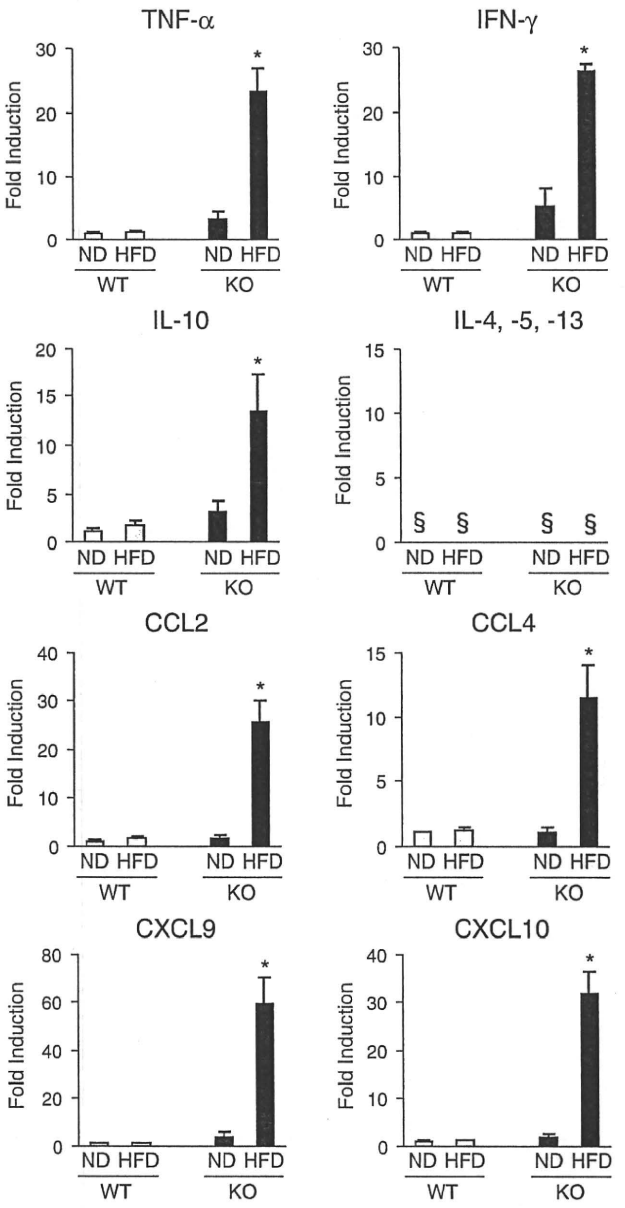

Fig. 3 Inflammatory cytokine and chemokine gene expression in the liver. Liver tissues were obtained from wild-type (*WT*) and Jα18-deficient (*KO*) mice fed either a normal diet (*ND*) or a high-fat diet (*HFD*) for 5 weeks. Liver RNA levels of the indicated genes and beta-actin as a control were analyzed using real-time reverse transcription polymerase chain reaction (RT-PCR). Data are shown as the fold increase of HFD-fed WT, ND-fed KO, or HFD-fed KO compared with ND-fed WT mice, with means ± SEM from five mice in each group. Data are representative of more than four independent experiments. *TNF-α* Tumor necrosis factor alpha, *IFN-γ* interferon gamma, *IL* interleukin, *CCL* chemokine (C–C motif) ligand, *CXCL* chemokine (C–X–C motif) ligand. §, not detected. *$P < 0.05$ versus KO fed ND

in the liver. Immunohistochemical examination revealed that CD4+ cells and CD8+ cells formed foci surrounding hepatocytes in the livers of KO mice (Fig. 4b), which partly corresponded to the inflammatory foci observed in the